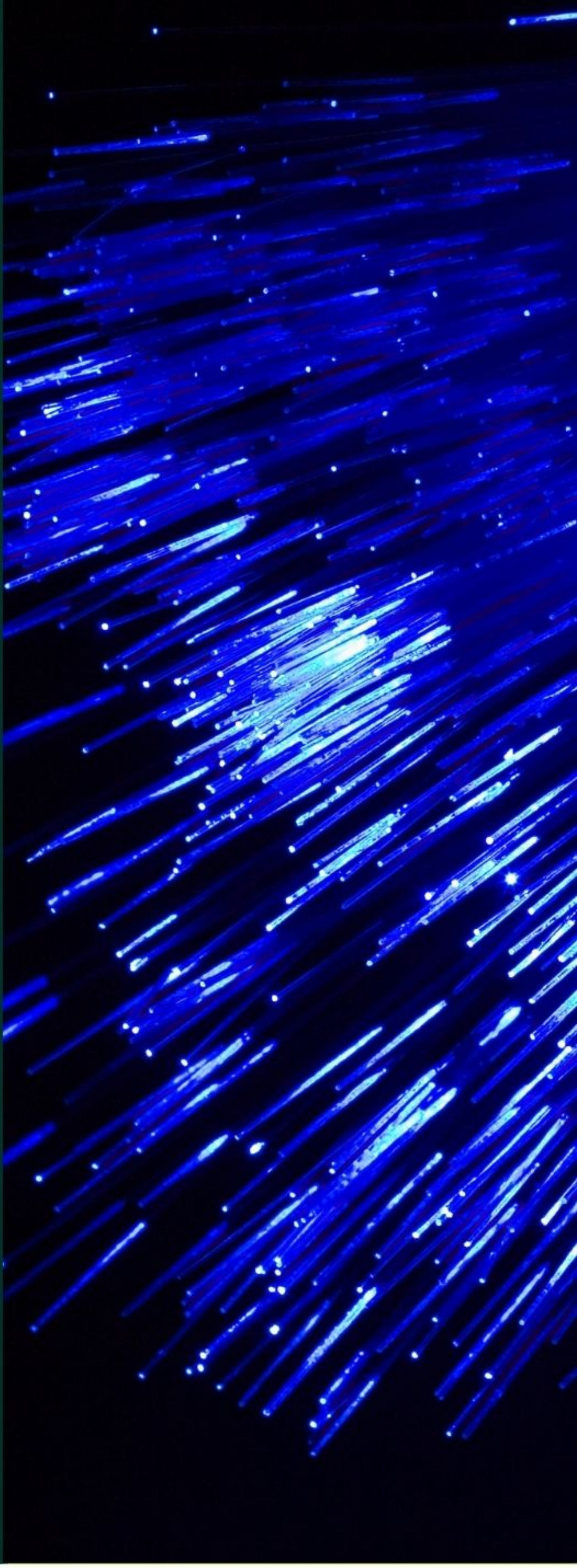

Received: 31 January 2023 | Revised: 26 March 2023 | Accepted: 1 June 2023

IET Optoelectronics

DOI: 10.1049/ote2.12097

The Institution of Engineering and Technology WILEY

ORIGINAL RESEARCH

Non-linear modelling and distortion compensation in optical Fast-orthogonal frequency division multiplexing systems

Luis Carlos Vieira[1,2] | Waseem Ozan[2] | John Mitchell[2] | Izzat Darwazeh[2]

[1]Graduate Program in Electrical and Computer Engineering (CPGEI), Federal University of Technology—Paraná (UTFPR), Curitiba, Brazil

[2]Department of Electronic and Electrical Engineering, University College London (UCL), London, UK

Correspondence

Luis Carlos Vieira.
Email: vieira@utfpr.edu.br

Abstract

Fast-OFDM-based intensity-modulation and direct-detection (IM/DD) has been proposed for deployment of cost-efficient optical access networks, due to its implementation simplicity and high spectral efficiency. In this article, the accuracy of the generalised memory polynomial (GMP) for the non-linear modelling of optical Fast-OFDM links is studied, including memory effects and considering different model parameters. After model validation using measured data of a 10 km single mode fibre link, the GMP is used for performance investigations of a distortion compensation approach to optical Fast-OFDM, for up to 16PAM modulation formats and different number of Fast-OFDM subcarriers. This study firstly reports the performance results of optical 16PAM-Fast-OFDM systems using either 2PAM- or 4PAM-based training signals for digital post-distortion and FFT-based channel estimation, and firstly investigates the influence of the zero padding (ZP) length on the performance of optical Fast-OFDM. Excellent performance improvements are achieved using the proposed distortion compensation scheme, relative to conventional system implementation.

KEYWORDS

intensity modulation, non-linear distortion, OFDM modulation, optical links

1 | INTRODUCTION

Optical intensity-modulation and direct-detection orthogonal frequency division multiplexing (IM/DD OFDM) is considered a promising solution for high data rate short-reach fibre-optic networks. It is a less complex and more suitable technique for cost-efficient deployment of optical access networks in comparison to coherent-detection optical OFDM systems [1, 2]. Nevertheless, in order to enable using quadrature amplitude modulation (QAM)-OFDM with IM/DD, Hermitian transpose is needed at the transmitter side to obtain a real signal at the output of inverse fast Fourier transform (IFFT) [1].

Fast-OFDM, proposed initially for wireless transmission in 2002 in ref. [3], is another multicarrier signal and system that has been used in many applications, including IM/DD optical systems [4–9], optical wireless communications [10, 11], and wireless systems [12–14]. Fast-OFDM advantageously offers either 50% bandwidth saving or double the number of data subcarriers within the same bandwidth compared to using conventional OFDM systems. This is achieved, respectively, by either compressing the frequency spacing between the subcarriers down to $1/2T$, where T is the symbol duration, or sampling faster in comparison to conventional OFDM. The reduction in inter-carrier spacing is beneficial in frequency selective links as it results in a flatter response per subcarrier [15]. In Fast-OFDM, the subcarriers are modulated with real data symbols using inverse discrete cosine transform (IDCT), and hence there is no need for Hermitian transpose at the transmitter. In addition, real-valued operation results in the reduction of implementation complexity and DSP power consumption. Thus, IM/DD Fast-OFDM can be considered an attractive solution for high-speed cost- and power-sensitive applications.

In IM/DD Fast-OFDM links, the non-linearity coming from the electro-optic converters may degrade the system performance. Fibre chromatic dispersion may also be an issue in the case of long-span links. In Mach–Zehnder modulator (MZM)-based IM/DD DC-offset Fast-OFDM systems, the

MZM is commonly biased at the quadrature point for best linearity [5]. Even at this bias, however, the high peaks of a Fast-OFDM signal may reach the non-linear region of the MZM characteristic. Moreover, MZMs suffer from the bias-drift problem [16]. Directed modulated distributed feedback laser (DML)-based optical Fast-OFDM links may also be used [6], but the DML non-linearity may cause significant waveform distortions [17]. Thus, the use of some linearisation and/or peak-to-average power ratio (PAPR) reduction approach might be necessary to alleviate the signal distortion issue.

Amplitude clipping is a simple approach to PAPR reduction of OFDM-based signals. This method, however, may cause additional in-band and out-of-band distortion [18]. Filtering after clipping can be used to reduce the out-of-band distortion. However, the non-linear distortion that falls within the signal bandwidth can not be filtered out [19]. Adaptive digital predistortion and post-distortion techniques have been proposed for the compensation of non-linear distortion in optical communication systems [4, 20–22]. Digital post-distortion represents a simpler solution than predistortion as the latter approach needs an additional feedback link for model identification. In addition, the non-linearity of the feedback link itself will reduce the predistortion performance [21].

In ref. [23], a FFT-based demodulation approach was proposed for Fast-OFDM systems, where zero padding (ZP) was used as the guard interval to counteract intersymbol interference (ISI). However, the reported researches using that Fast-OFDM approach for direct-detection optical links [4, 5, 9] have not considered the effect of changing the length of ZP on the system performance.

In ref. [24], a generalised memory polynomial (GMP) was proposed for digital predistortion of RF power amplifiers. The GMP model combines the basic memory polynomial (MP) structure [25] with cross terms between the signal and lagging and/or leading exponentiated envelope terms, which makes the GMP more effective in modelling and compensating the system dynamic non-linearity compared to the MP model.

This paper is an extension of the authors' conference paper reported in ref. [26] related to non-linear modelling and distortion compensation in optical Fast-OFDM systems. In ref. [26], the GMP was firstly employed to model the dynamic non-linearity of direct-detection optical Fast-OFDM links. After model validation using measured data from a 10-km optical link, the GMP-based optical Fast-OFDM model was applied for the performance investigation of a combined amplitude clipping and digital post-distortion scheme. In addition, two-level pulse amplitude modulation (2PAM)-based training signals were firstly proposed for the distortion compensation and FFT-based channel estimation of optical 8PAM-Fast-OFDM systems, with significant BER improvements reported. In the present paper, the following issues are added to the aforementioned conference paper:

- An analysis of system's non-linear distortion.
- The influence of changing cross-term parameters on the GMP model accuracy.
- An investigation of the length of ZP-type guard interval on the performance of optical Fast-OFDM links.
- A performance comparison of the compensation scheme using 2PAM versus 4PAM-based training signals, and considering different number of training symbols.
- First performance results of optical 16PAM-Fast-OFDM using the proposed distortion compensation approach.

2 | SIGNAL MODEL AND SYSTEM DESCRIPTION

The discrete time Fast-OFDM signal $x(n)$, generated based on IDCT, is defined as

$$x(n) = \sqrt{\frac{2}{N}} \sum_{k=0}^{N-1} \epsilon(k) s(k) \cos\left[\frac{\pi(2n+1)k}{2N}\right] \quad (1)$$

where N is the number of subcarriers, $n = \{0, 1, \ldots, N-1\}$ is the time sample index in a Fast-OFDM symbol, and $s(k)$ is the real-valued data symbol carried by the kth subcarrier, and $\epsilon(k) = \sqrt{0.5}$ for $k = 0$ and 1 for $k = \{1, 2, \ldots, N-1\}$.

In Figure 1, the block diagram of the proposed IM/DD Fast-OFDM system is shown. At the transmitter side, the input data are PAM mapped and then, in the IDCT block, modulated on each Fast-OFDM subcarrier. After that, the ZP is added to each Fast-OFDM symbol as guard interval. Then, amplitude clipping is used for PAPR reduction, followed by digital-to-analog conversion (DAC). The analog Fast-OFDM signal is then electrical amplified and transmitted over the IM/DD link. In this work, a 1550-nm DFB laser source and a single-drive MZM are used as optical transmitter. The MZM is connected to a 50-GHz PIN photodiode via a 10 km single mode optical fibre (SMF). Alternatively, as optical transmitter, DMLs or electro-absorption modulated lasers (EMLs) can also be used. At the receiver side, the photo-detected signal is amplified and, after analog-to-digital conversion, downloaded to MATLAB for offline processing. The following receiver DSP

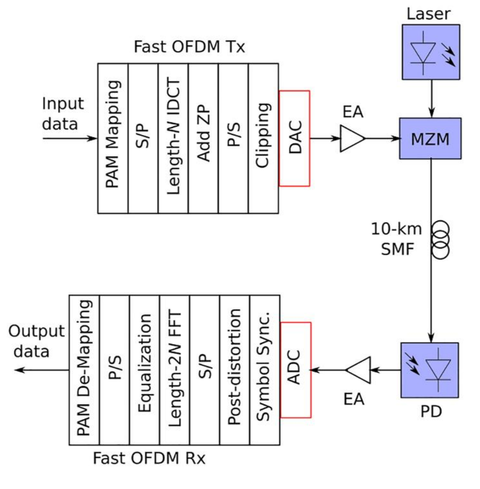

FIGURE 1 Diagram of the IM/DD Fast-OFDM system.

functions are employed: symbol synchronization (time alignment), digital post-distortion, Fast-OFDM demodulation based on a length-2N FFT approach [23], channel estimation and zero-forcing equalisation, and PAM de-mapping.

3 | ANALYSIS OF NON-LINEAR DISTORTION

In this Section, the non-linear distortion of the MZM-based IM/DD Fast-OFDM system is analysed based on a derivation previously introduced for optical OFDM [27].

At the MZM output, the double side-band optical Fast-OFDM signal is given by

$$E_o(t) = \cos\left[\frac{\pi}{2V_\pi}(V_b + x(t))\right]\sqrt{P_i}\cos(2\pi f_o t) \tag{2}$$

where $x(t)$ is the continuous time Fast-OFDM modulating signal, V_b is the bias voltage, $V\pi$ is the MZM half-wave voltage, P_i is the power level of the optical carrier at the MZM input, and f_o is the optical carrier frequency.

For simplicity, impairments due to optical fibre + dispersion are neglected. This is a reasonable assumption for short-reach IM/DD links. In this work, the application of our compensation scheme for long-span optical links is not considered. At the receiver, the output current $i_o(t)$ of the photodiode with responsivity R is calculated by squaring the modulus of $E_o(t)$ as follows

$$\begin{aligned} i_o(t) &= RP_i\cos^2\left[\frac{\pi}{2V_\pi}(V_b + x(t))\right] \\ &= \frac{RP_i}{2}\left[1 + \cos\left(\frac{\pi V_b}{V_\pi} + \frac{\pi x(t)}{V_\pi}\right)\right] \\ &= \frac{RP_i}{2}\left[1 + \cos\left(\frac{\pi V_b}{V_\pi}\right)\cos\left(\frac{\pi x(t)}{V_\pi}\right)\right. \\ &\qquad \left. - \sin\left(\frac{\pi V_b}{V_\pi}\right)\sin\left(\frac{\pi x(t)}{V_\pi}\right)\right] \end{aligned} \tag{3}$$

If the MZM bias voltage is set at the quadrature point ($V_b = \pm V_\pi/2$) the Equation (3) can be simplified as

$$i_o(t) = \mp\frac{RP_i}{2}\sin\left(\frac{\pi x(t)}{V_\pi}\right) + \frac{RP_i}{2} \tag{4}$$

Using the Taylor series, $i_o(t)$ can be expanded with respect to $x(t)$ as follows

$$\begin{aligned} i_o(t) = \frac{RP_i}{2}&\left[1 \mp \left(\frac{\pi x(t)}{V_\pi}\right) \pm \left(\frac{\pi x(t)}{V_\pi}\right)^3 \Big/ 3!\right. \\ &\left. \mp \left(\frac{\pi x(t)}{V_\pi}\right)^5 \Big/ 5! \pm \ldots\right] \end{aligned} \tag{5}$$

Equation (5) shows a linear term in $x(t)$ followed by third- and fifth-order distortion terms. Thus, for $V_b = \pm V_\pi/2$ and assuming ideal MZM transfer characteristic, the even-order distortion can be eliminated. In addition, if a small Fast-OFDM signal drives the MZM the high odd-order distortion will be insignificant.

Considering now the MZM bias of $V_b = \pm V_\pi$. For this case, Equation (3) becomes

$$i_o(t) = -\frac{RP_i}{2}\cos\left(\frac{\pi x(t)}{V_\pi}\right) + \frac{RP_i}{2} \tag{6}$$

Then, after Taylor series expansion, $i_o(t)$ is given by

$$i_o(t) = \frac{RP_i}{2}\left[\left(\frac{\pi x(t)}{V_\pi}\right)^2 \Big/ 2! - \left(\frac{\pi x(t)}{V_\pi}\right)^4 \Big/ 4! + \ldots\right] \tag{7}$$

There are only even-order non-linear terms in Equation (7), which shows that the original (non-distorted) signal cannot be recovered after direct photodetection and, therefore, the bias voltage cannot be set exactly at $\pm V_\pi$ for such IM/DD system.

Usually, in MZM-based IM/DD DC-offset Fast-OFDM systems, low input signal power is used and the MZM is biased at $V_b = \pm V_\pi/2$, for best linearity. This, however, results in low system sensitivity as the optical carrier's power is higher than the power in the sidebands and the optical carrier itself transmits no information. The sensitivity can be improved by increasing the input signal power. However, high amplitude input signals suffer from non-linear distortion.

The strategy in our IM/DD Fast-OFDM system is to set $V_b = \pm V_\pi/2$ and to use high input signal power levels, with the additional signal distortion reduced by using the proposed non-linear compensation scheme. In this way, an IM/DD Fast-OFDM system with high sensitivity and low distortion can be obtained.

4 | MODELLING AND COMPENSATION APPROACHES

4.1 | Modelling approach

In this work, a behavioural modelling approach is adopted to obtain the non-linear models. With this approach, the model coefficients are extracted using input-output time-domain measured data and classical parameter estimation theory [28]. The measured data for the model extraction comes from the transmission of a 1.87 GHz Fast-OFDM signal over a 10 km length direct-detection optical link as described in ref. [29], with the addition of an RF amplifier after the photodiode. A Fast-OFDM signal with IDCT size of 512 and 192 data subcarriers is used for model estimation only. Each data subcarrier is modulated by 4PAM symbols. More details on the measurement setup can be found in ref. [29]. In MATLAB, the baseband Fast-OFDM input-output signals are firstly time aligned and then the coefficients of the GMP model are obtained using the least-squares method, which estimates coefficients by minimising the summed square of residuals. The output y_{GMP} of the GMP model is related to its input x by:

$$\begin{aligned} y_{GMP}(n) = &\sum_{k=1}^{K_a}\sum_{q=0}^{Q_a} a_{kq}x(n-q)|x(n-q)|^{k-1} \\ &+\sum_{k=2}^{K_b}\sum_{q=0}^{Q_b}\sum_{m=1}^{M_b} b_{kqm}x(n-q)|x(n-q-m)|^{k-1} \\ &+\sum_{k=2}^{K_c}\sum_{q=0}^{Q_c}\sum_{m=1}^{M_c} c_{kqm}x(n-q)|x(n-q+m)|^{k-1} \end{aligned} \quad (8)$$

Here, the first polynomial function is applied to time-aligned input signal samples, where K_a and Q_a are the non-linearity order and the memory depth respectively. The second polynomial function introduces cross-terms between the complex input signal and its lagging envelope terms up to the order of M_b and has a non-linearity order K_b and memory depth of Q_b. The third polynomial introduces leading cross-terms up to the order of M_c and has a non-linearity order and memory depth of K_c and Q_c respectively. The parameters a_{kq}, b_{kqm}, and c_{kqm} are the coefficients of the GMP model for the aligned terms, and the lagging and leading cross-terms respectively. In this work, we use only odd-order non-linear terms in the GMP model. It should be noted that, although the GMP is a non-linear model, all of its coefficients can be easily estimated using any least-squares algorithm [24].

Using the same measured data, we also obtain a MP-based optical Fast-OFDM model for comparison with the accuracy of the GMP model. The MP model is given by

$$y_{MP}(n) = \sum_{k=1}^{K}\sum_{q=0}^{Q} a_{kq}x(n-q)|x(n-q)|^{k-1} \quad (9)$$

where $x(n-q)$ is the input signal delayed by q sample periods, K is the non-linearity order, Q is the memory length, and a_{kq} are the model coefficients. For a fair comparison with the GMP model, we use only odd-order non-linear terms in the MP model. The GMP and MP model training procedure is based on the least-squares method and is summarised below, following the derivation in ref. [30].

All memory-polynomial based models can be described using a generic vector format given by

$$y(n) = \mathbf{U}(n)\mathbf{A} \quad (10)$$

where $\mathbf{U}(n)$ is a vector constructed using the baseband input signal samples according to the basis functions of the GMP or MP model, and $\mathbf{A}$ is the vector containing the corresponding model coefficients. For a set of N samples, the GMP (or MP) model can be compactly expressed as

$$\widehat{y} = \mathbf{XA} \quad (11)$$

where $\widehat{y}$ is an N x 1 vector that represents an estimate of the actual output vector $\mathbf{y}$, and $\mathbf{X}$ is a matrix whose rows are delayed versions of $\mathbf{U}(n)$, given by

$$\mathbf{X} = [\mathbf{U}(n)\ \mathbf{U}(n-1)\ \ldots \mathbf{U}(n-N+1)]^T \quad (12)$$

For a block of N samples, the estimation error (in vector form) is $\mathbf{e} = \mathbf{y} - \widehat{y}$. The model coefficients can be obtained by applying the least-squares solution to minimise the mean squared error, as follows

$$\mathbf{A} = \left(\mathbf{X}^H\mathbf{X}\right)^{-1}\mathbf{X}^H\mathbf{y} \quad (13)$$

It should be noted that the GMP and MP models were trained using the measured data from the 10 km IM/DD link operating in a certain degree of non-linearity. In simulation, the GMP/MP models can be applied for performance investigations considering different input signal parameters, assuring that the input signal does not extrapolate the signal amplitude and bandwidth used for the model extraction.

4.2 | Distortion compensation approach

The block diagram of the distortion compensation scheme for IM/DD Fast-OFDM links is depicted in Figure 2. In this work, a simple amplitude clipping method (without filtering) is used. The clipped version $x_c(n)$ of the Fast-OFDM signal $x(n)$ is given by

$$x_c(n) = \begin{cases} x(n) & \text{if } |x(n)| \le A_{th}, \\ A_{th}e^{j\theta} & \text{if } |x(n)| > A_{th}. \end{cases} \quad (14)$$

where $\theta = \arg[x(n)]$, and A_{th} is the amplitude threshold. The phase of $x(n)$ is not altered by the clipping function. By setting A_{th} to a lower value than the peak amplitude $A_{\max}$ of $x(n)$, the PAPR of the Fast-OFDM signal is reduced. Here, we define a clipping factor $CF = A_{th}/A_{\max}$.

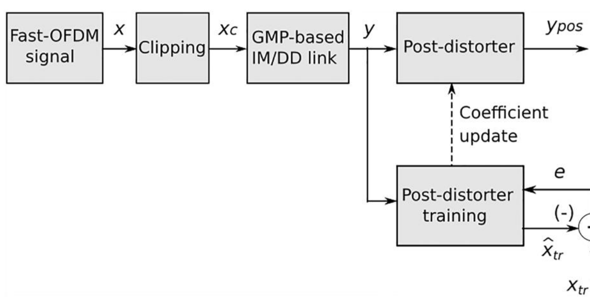

FIGURE 2 The distortion compensation approach.

As shown in Figure 2, the digital post-distorter is inserted after the IM/DD link (in baseband). It is trained for executing the inverse function of the optical link non-linearity so that the complete system is linearised. As post-distorter model, we use a simple memoryless polynomial function. The GMP model is not chosen as post-distorter due to its high complexity for real-time implementation. The post-distorter coefficients are obtained using known PAM-Fast-OFDM training sequences and a least squares (LS) fitting algorithm, provided by the "polyfit" function in MATLAB. High amplitude training signals, capable of sweeping all the link non-linear characteristic, are used. In the diagram of Figure 2, the post-distorter coefficients are estimated by minimising the error e between the reference training signal x_{tr} and the post-distorter training block output $\hat{x}_{\text{tr}}$. The estimated coefficients are then used to update the actual post-distorter. The post-distorted signal y_{pos} is then sent to the FFT-based demodulation and equalisation, followed by PAM de-mapping.

In Figure 2, the output y_{pos} of the memoryless polynomial-based digital post-distorter is defined by

$$y_{pos}(n) = \sum_{k=0}^{K} a_k y(n)^k \tag{15}$$

where $y(n)$ is the baseband received signal, a_k are the model coefficients, and K is the polynomial order. In (15), we include both odd- and even-order non-linear terms and set K to 3.

In this work, we adopt a block-based post-distortion training approach. With this approach, the training can be done in only one step and in a least-squares sense, avoiding the use of sample-by-sample algorithms. In addition, as previously proposed in ref. [4], the received training signals are also post-distorted before being used for the FFT-based channel estimation and equalisation. In this way, the memoryless polynomial based post-distortion approach has also a dynamic compensation effect on the system performance.

After post-distortion, the signal is serial-to-parallel converted and fed to the FFT block (see Figure 1) for Fast-OFDM demodulation. Then, the frequency domain channel estimation is realized for the data subcarriers based on known PAM-Fast-OFDM training symbols. In this work, a block-type channel estimation approach is adopted in which reference PAM symbols are inserted into all subcarriers of Fast-OFDM training symbols. The channel response of each subcarrier is estimated as

$$H(k) = \frac{y_{TS}(k)}{x_{TS(k)}} \tag{16}$$

where $y_{TS}(k)$ and $x_{TS}(k)$ are the kth frequency component of the received training symbol and the known (reference) training symbol respectively. The actual channel frequency response is obtained by averaging over a sequence of training symbols. After channel estimation, the received signal is phase compensated and its real part is extracted. Then, the transmitted PAM signal is obtained using single-tap equalisation.

5 | MODELLING AND PERFORMANCE RESULTS

5.1 | Modelling accuracy

The accuracy of the GMP model is now compared against that of the MP model, using the normalised mean square error (NMSE) as performance metric. The same Fast-OFDM measured data are used to estimate the GMP and MP model coefficients.

In Table 1, a first set of accuracy results is presented. For these results, we proportionally increase the number of coefficients in both models by changing K_a and Q_a in (8) and K and Q in (9). The other GMP model parameters are fixed at: $K_b = 3$, $Q_b = 1$, $M_b = 1$, $K_c = 5$, $Q_c = 4$, and $M_c = 4$. For memory length $Q_a = 10$ or more and similar number of coefficients, the GMP model achieves better accuracy than the MP model. For $Q_a = 20$, the NMSE of the GMP model is around 2 dB less than that of the MP model.

For the second set of NMSE results, shown in Table 2, K_a and Q_a are set to 3 and 20, respectively, and the memory depth Q_c of the leading cross-terms in Equation (8) is changed. The remaining GMP parameters are fixed at: $K_b = 3$, $Q_b = 2$, $M_b = 1$, $K_c = 5$, and $M_c = 4$. For the MP model, we keep $K = 3$ and vary Q to obtain the same number of coefficients as the GMP model. From Table 2, we can observe that the accuracy of the GMP model improves from around −26.2 dB to −26.7 dB when Q_c increases from 6 to 12. In contrast, the MP accuracy is almost the same for similar increase in the number

TABLE 1 Modelling accuracy.

GMP model				MP model			
Ka	Qa	No. Coeffs.	NMSE (dB)	K	Q	No. Coeffs.	NMSE (dB)
3	5	45	−22.44	3	22	46	−23.84
3	10	55	−25.30	3	27	56	−23.86
3	15	65	−25.90	3	32	66	−23.97
3	20	75	−25.95	3	37	76	−23.87
5	5	51	−22.46	5	16	51	−23.94
5	10	66	−25.33	5	21	66	−23.97
5	15	81	−25.94	5	26	81	−23.99
5	20	96	−25.98	5	31	96	−24.01

TABLE 2 Modelling accuracy.

GMP model			MP model		
Qc	No. Coeffs.	NMSE (dB)	Q	No. Coeffs.	NMSE (dB)
6	92	−26.22	45	92	−23.87
8	108	−26.50	53	108	−23.88
10	124	−26.62	61	124	−23.88
12	140	−26.67	69	140	−23.89

of model coefficients. For $Q_c = 12$ and 140 coefficients, the NMSE of the GMP model is around 2.8 dB better than that of the MP model.

In Figure 3, the measured and GMP modelled time-domain Fast-OFDM signals are presented, while the MP modelled signal is shown in Figure 4. It can be seen that a better agreement between the measured and modelled signals is obtained using the GMP model.

5.2 | Non-linearity compensation and IDCT size

In this Section, a performance investigation of the proposed distortion compensation scheme for MZM-based IM/DD Fast-OFDM links and for different IDCT sizes is reported. The Fast-OFDM signal has a bandwidth of about 1.87 GHz and an average power level of 13.5 dBm (before clipping). The clipping factor (CF) is set to 0.8. 2PAM-based training sequences (TS) are used for both post-distortion training and frequency domain channel estimation. In the post-distorter model of Equation (15), K is set to 3. The GMP model parameters in Equation (8) are as follows: $K_a = 3$, $Q_a = 15$, $K_b = 3$, $Q_b = 1$, $M_b = 1$, $K_c = 5$, $Q_c = 4$, and $M_c = 4$. The total number of GMP coefficients is 65.

In Figure 5, the BER results for a 10 km length IM/DD 4PAM-Fast-OFDM link with and without the proposed compensation approach are shown, for the IDCT sizes N of 64, 128, and 256. A 2PAM TS with length of 10 symbols is employed. The amount of data subcarriers is augmented proportionally from 24 to 96 in order to maintain the same signal bandwidth and bit rate for the three IDCT cases. The length of the ZP corresponds to 1/32 of the IDCT size. For each N-size IDCT, a post-distorter training signal with same IDCT size is used. The performance of the 4PAM-Fast-OFDM with distortion compensation is significantly improved compared to the conventional system implementation. For example, at a BER level of 10^{-3}, the required SNR is reduced by around 3 dB and almost 5 dB due to the distortion compensation, for the IDCT sizes of 128 and 64 respectively. From Figure 5, it can also be seen that the BER performance improves with increasing N. This is due to the reduction in the bandwidth of Fast-OFDM subcarriers, which enhances the performance of the frequency domain equalisation. The BER performances of the proposed post-distortion approach for 8PAM-Fast-OFDM signals using the same 10 km length SMF-based GMP model and for the IDCT sizes of 64, 128, and 256 were reported in ref. [26], in which the BER improvement with increasing IDCT size was also observed.

5.3 | 2PAM versus 4PAM training signals for 8PAM/16PAM-fast-OFDM

In this Section, a comparison of the distortion compensation performance using 2PAM and 4PAM-based training sequences (TS) and considering different TS lengths are presented and discussed. The performances are evaluated for 8PAM- and 16PAM-Fast-OFDM data signals with IDCT size of 256, ZP size of 8, and Eb/No of 26 dB. No clipping is used as the

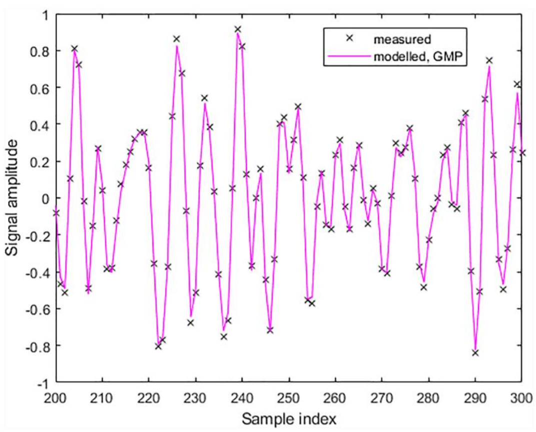

FIGURE 3 Fast-OFDM signal modelling result. GMP model, 108 coefficients.

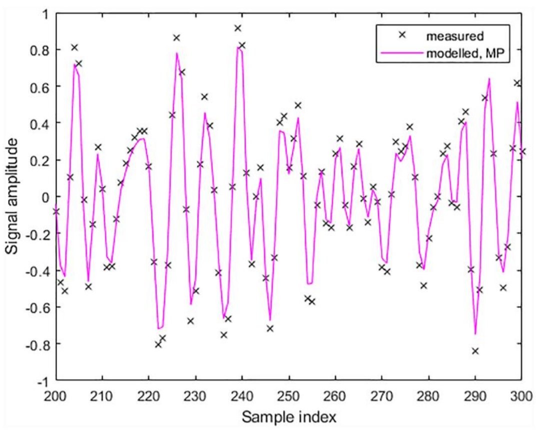

FIGURE 4 Fast-OFDM signal modelling result. MP model, 108 coefficients.

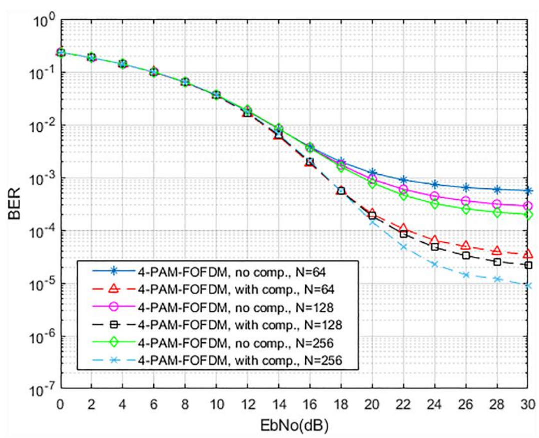

FIGURE 5 BER performances with/without distortion compensation for the optical 4PAM-Fast-OFDM with different IDCT sizes (N). TS = 10.

8PAM/16PAM signals are very sensitive to the clipping-induced distortion. The average power levels of the input 8PAM- and 16PAM-Fast-OFDM signals are 10.5 dBm and 7.5 dBm respectively. Here, the same GMP and post-distorter model parameters (as described in Section 5.2) are used.

The BER results for the 8PAM-Fast-OFDM link are shown in Figure 6. It can be observed that the 2PAM outperforms the 4PAM training signal, especially for low number of training symbols and with distortion compensation. For example, BER levels of below 1×10^{-4} and below 2×10^{-5} are obtained by using 6 (or more) training symbols and with distortion compensation for the 4PAM- and 2PAM-based training cases respectively. With the 4PAM training signal, a BER level just below 2×10^{-5} is achieved if at least 14 training symbols are used. This means a reduction of around 57% in the TS length (an increase in net bit rate) by using the 2PAM instead of 4PAM training signal.

In Figure 7, the performance results for the 16PAM-Fast-OFDM system are presented. For most of the TS lengths, a better performance is achieved with the 2PAM-than the 4PAM-based training, and the performance differences are clearly more significant when the compensation approach is employed. For example, for the distortion compensated results, BER levels below 3×10^{-4} are achieved if at least 10 and 18 training symbols are used for the 2PAM- and 4PAM-based training cases respectively. This means a reduction of 44.4% in the TS length by using 2PAM compared to 4PAM training signal. It is important to note that the 16PAM-Fast-OFDM requires a longer TS in comparison to the 8PAM-Fast-OFDM to achieve the lowest BER level.

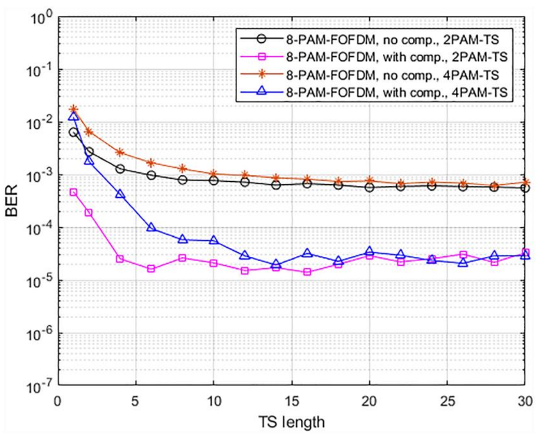

FIGURE 6 BER performances with/without distortion compensation versus TS length for the optical 8PAM-Fast-OFDM. $N = 256$.

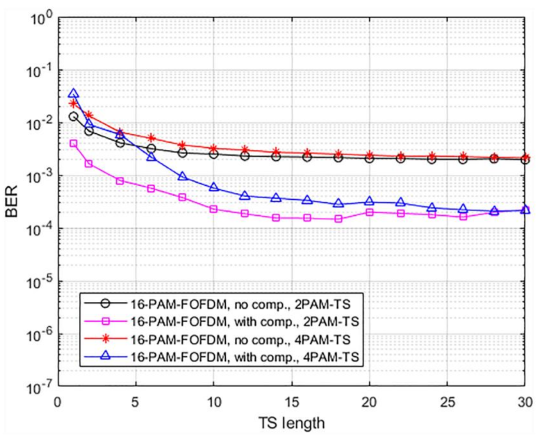

FIGURE 7 BER performances with/without distortion compensation versus TS length for the optical 16PAM-Fast-OFDM. $N = 256$.

5.4 | Non-linearity compensation for different ZP lengths

We now investigate the performance of the post-distortion approach for 8PAM-Fast-OFDM and 16PAM-Fast-OFDM signals considering the ZP lengths of 2, 4 and 8. The IDCT size of 256 and 2PAM TS with length of 10 symbols are used. The same 10 km length SMF-based GMP and post-distorter models are used, as previously described. No clipping is employed.

The performance results for the 8PAM-Fast-OFDM link are shown in Figure 8. The input signal power level is 10.5 dBm. Similar performances are obtained for the three ZP length cases, with a small difference in favour of ZP = 2 at the higher Eb/No region. At the BER of 1×10^{-3}, Eb/No gains of more than 4 dB are achieved with post-distortion in comparison to the conventional Fast-OFDM, for the three ZP length cases. Thus, considering the 8PAM-Fast-OFDM, the ZP length of 2 would be the best choice to achieve a higher net bit rate.

The BER results for the 16PAM-Fast-OFDM are presented in Figure 9. The BER for ZP = 8 is sligthly better than that for ZP = 4 and significantly better than that for ZP = 2. At the BER level of 1×10^{-3}, for example, an Eb/No gain of almost 6 dB is achieved with the distortion compensation approach in comparison to the conventional 16PAM-Fast-OFDM, for ZP of either 4 or 8. Thus, for higher net bit rate

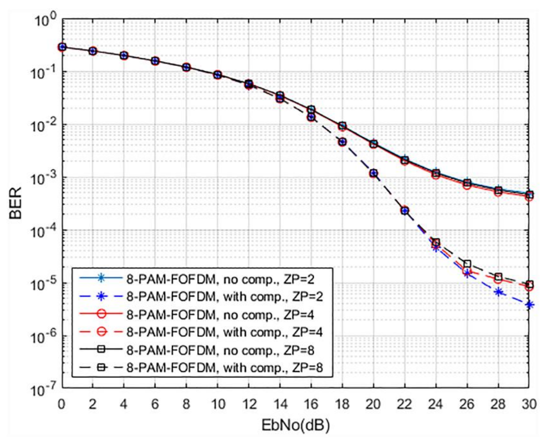

FIGURE 8 BER performances with/without distortion compensation for the optical 8PAM-Fast-OFDM with different ZP sizes. $N = 256$, TS = 10.

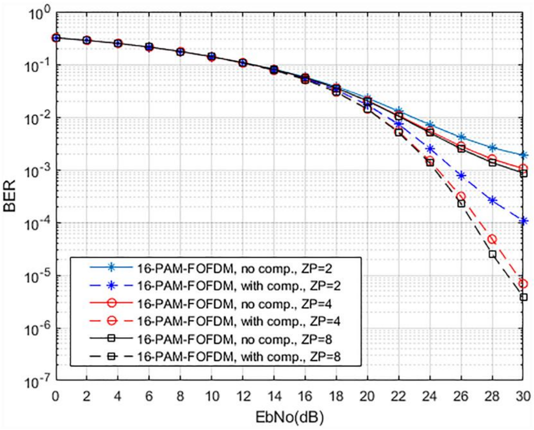

FIGURE 9 BER performances with/without distortion compensation for the optical 16PAM-Fast-OFDM with different ZP sizes. $N = 256$, TS = 10.

and good performance, the ZP length of 4 would be a reasonable choice.

A bit rate of around 15 Gbit/s can be achieved with the 16PAM-Fast-OFDM signal and for the sampling rate of 10 GS/s, as used in our measurement setup. The link data rate can be further increased by using higher number of data subcarriers (for a given IDCT size), but this would occupy a wider bandwidth. It is worth noting that the performance improvement with our memoryless polynomial based post-distorter should become less significant for very high bandwidth signals due to the expected increase in the system's memory effects, and further investigations on the bandwidth limit of the compensation approach are still needed.

In Figure 10, the 8PAM received signal constellations after the 10 km IM/DD link, obtained using 10 training symbols and for $N = 256$, are shown. It can clearly be observed the improvement in the signal constellation when the proposed digital compensation scheme is applied to the optical Fast-OFDM link. For the sake of visualisation, the constellations are plotted including the real and imaginary signal components obtained after the equalisation block in the receiver diagram (see Figure 1). The PAM de-mapping block will recover only the real part of the equalised signal.

5.5 | Fast-OFDM versus OFDM performances

Transmission performance comparisons between optical Fast-OFDM and OFDM are now presented using the same post-distorter and GMP parameters of Section 5.2. Both multi-carrier signals are set with the average power of 13.5 dBm and have the bandwidth of 1.87 GHz. A clipping factor of 0.8 is used. 2PAM- and 4QAM-based training sequences are used for the optical Fast-OFDM and OFDM link cases respectively.

In Figure 11, the BER results with/without distortion compensation for optical 4PAM-Fast-OFDM and 16QAM-OFDM systems are compared, for $N = 64$ and TS = 10. The

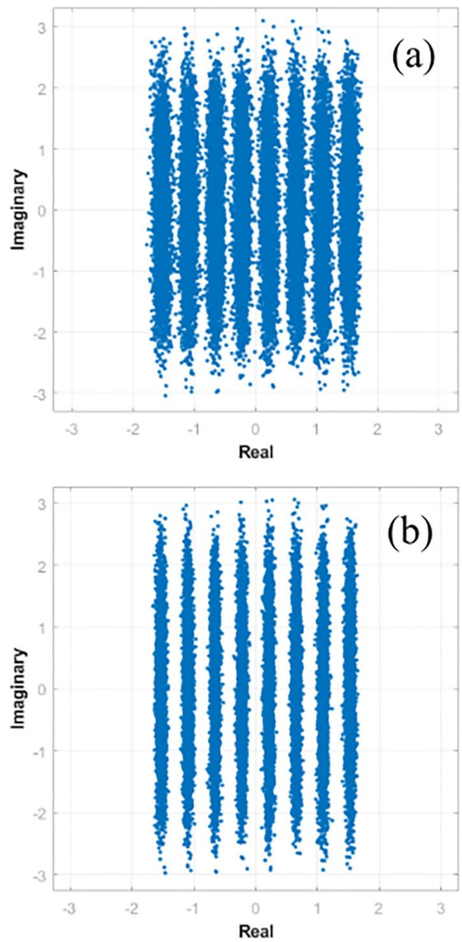

FIGURE 10 8PAM received constellations for $N = 256$: (a) without distortion compensation, (b) with distortion compensation.

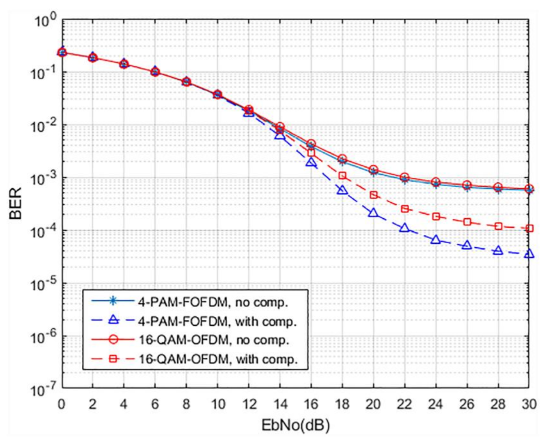

FIGURE 11 BER performances with/without distortion compensation for 4PAM-Fast-OFDM and 16QAM-OFDM IM/DD systems. $N = 64$, TS = 10.

ZP and cyclic prefix (CP) lengths of the Fast-OFDM and OFDM signals, respectively, are set to 2. The performances of the two systems are evaluated using GMP-based optical Fast-OFDM and OFDM link models. Both link models have the

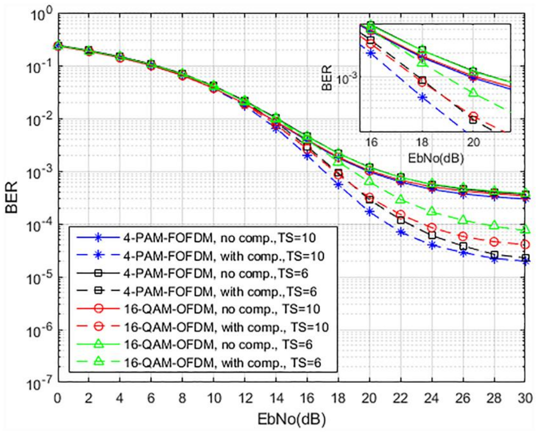

FIGURE 12 BER performances with/without distortion compensation for 4PAM-Fast-OFDM and 16QAM-OFDM IM/DD systems. $N = 128$.

same structure and number of coefficients and were extracted from the same 10 km SMF link. The bit rates of the 4PAM-Fast-OFDM and the 16QAM-OFDM links are equal. Considering the results without compensation, the performances of the two multicarrier systems are very similar. With distortion compensation, however, the 4PAM-Fast-OFDM outperforms the 16QAM-OFDM at the higher Eb/No region. The reason for this is that the bandwidth of the Fast-OFDM subcarrier is half of that of the OFDM one, and hence the level of memory effect per subcarrier is lower for the Fast-OFDM link. As previously stated (in Section 5.4), our memoryless-based post-distorter works better for low bandwidth signals.

In Figure 12, the BER performances of the 4PAM-Fast-OFDM and 16QAM-OFDM are compared, with N set to 128 and the TS length set to 6 and 10. These results are obtained using the ZP and CP lengths of 2. With distortion compensation, the 4PAM-Fast-OFDM performs better than the 16QAM-OFDM at the higher Eb/No region, for both TS cases. For the results with TS = 6, at the BER of 1×10^{-3}, Eb/No gains of about 3 and 2 dB are obtained due to distortion compensation for the 4PAM-Fast-OFDM and 16QAM-OFDM links respectively. Similarly, for the case of TS = 10 and at the same BER value, Eb/No gains of about 3 and 2.2 dB are achieved due to distortion compensation for the 4PAM-Fast-OFDM and 16QAM-OFDM respectively. In addition, for the 4PAM-Fast-OFDM with compensation, the required Eb/No is reduced by almost 1 dB for the 10-TS compared to 6-TS case (at BER = 10^{-3}). However, the net bit rate of the 6-TS case will be higher.

6 | CONCLUSION

In this paper, we study the accuracy of the GMP for the modelling of non-linear and memory effects of optical Fast-OFDM links, considering different values of parameters in the GMP model structure. In addition, we investigate the influence of ZP length on the BER performance of our previously proposed distortion compensation scheme for optical Fast-OFDM systems [20]. We also include a performance comparison of 2PAM-versus 4PAM-based training signals. Moreover, this is the first time that our distortion compensation approach is applied to optical 16PAM-Fast-OFDM links, with excellent BER improvements reported.

The GMP-based modelled Fast-OFDM signal shows an excellent agreement with the measured time-domain signal. In comparison to the MP model, for similar number of coefficients, better modelling accuracy is obtained using the GMP model for most of the reported results. For the highest number of model coefficients, the NMSE of the GMP model is about 2.8 dB better than that achieved with the MP model.

The BER results show that the combination of clipping and digital post-distortion can significantly improve the system performance of a 10 km SMF IM/DD 4PAM-Fast-OFDM link, with an Eb/No gain of almost 5 dB achieved (at a BER of 1×10^{-3}) in comparison to conventional optical Fast-OFDM. At the same BER value, for the 8PAM-Fast-OFDM link and $N = 256$, an Eb/No gain of more than 4 dB is achieved due to the proposed compensation approach and no significant performance difference is reported by comparing the ZP-length cases of 2, 4 and 8. For the case of 16PAM-Fast-OFDM and $N = 256$, the best compensation performance is obtained for the ZP length of 8, with an Eb/No gain of almost 6 dB achieved (at the BER of 1 x 10^{-3}) in comparison to conventional optical Fast-OFDM. In addition, a better distortion compensation performance is achieved by using 2PAM than 4PAM training signal. The BER results show that the length of the training sequence can be significantly reduced by using 2PAM-instead of 4PAM-based training, with reductions of more than 55% and 44% reported for the 8PAM and 16PAM-Fast-OFDM link cases.

The BER performances of the IM/DD Fast-OFDM and conventional OFDM systems with and without clipping/post-distortion have also been compared, for the IDCT sizes of 64 and 128 and the TS lengths of 6 and 10. The results show that the 4PAM-Fast-OFDM system performs better than the 16QAM-OFDM due to the distortion compensation scheme and at the higher Eb/No region. We highlight that, even when the optical Fast-OFDM and OFDM achieve similar BER results, the Fast-OFDM system is less complex to implement. As future work, the limits of application of the proposed compensation scheme in terms of data rate and transmission distance should be investigated.

AUTHOR CONTRIBUTION

Luis Carlos Vieira: Conceptualisation, Methodology, Software, Investigation, Writing - original draft, Writing - review and editing. **Waseem Ozan**: Software, Writing - review and editing. **John Mitchell**: Writing - review and editing. **Izzat Darwazeh**: Supervision, Writing - review and editing.

ACKNOWLEDGEMENTS

Luis C. Vieira would like to thank the support from the Department of Electronics (DAELN), Federal University of Technology—Paraná (UTFPR), Brazil.

CONFLICT OF INTEREST STATEMENT

None.

DATA AVAILABILITY STATEMENT

Research data are not shared.

ORCID

Luis Carlos Vieira https://orcid.org/0000-0003-4531-4428

REFERENCES

1. Ma, J., et al.: Enhanced performance of PS-256QAM-OFDM for optical access network. Opt Commun. 467, 125566 (2020). https://doi.org/10.1016/j.optcom.2020.125566
2. Zou, D., et al.: Comparison of bit-loading DMT and pre-equalized DFT-spread DMT for 2-km optical interconnect system. J. Lightwave Technol. 37(10), 2194–2200 (2019). https://doi.org/10.1109/jlt.2019.2899737
3. Rodrigues, M.R.D., Darwazeh, I.: Fast OFDM: a proposal for doubling the data rate of OFDM schemes. In: Proc. IEEE/IEE Int. Conf. Telecommun. (2002)
4. Vieira, L.C., et al.: A combined digital linearization and channel estimation approach for IM/DD fast-OFDM systems. Opt. Fiber Technol. 67, 102725 (2021). https://doi.org/10.1016/j.yofte.2021.102725
5. Zhou, Z., et al.: Experimental demonstration of an SFO-robustness scheme with fast OFDM for IMDD passive optical network systems. J. Lightwave Technol. 38(20), 1–5616 (2020). https://doi.org/10.1109/jlt.2020.3004429
6. Zhou, Z., et al.: Adaptive modulation scheme for DML-based IM/DD FOFDM systems using overlap frequency-domain equalization. Opt. Fiber Technol. 48, 213–217 (2019). https://doi.org/10.1016/j.yofte.2019.01.011
7. Giacoumidis, E., et al.: Experimental and theoretical investigations of intensity-modulation and direct-detection optical fast-OFDM over MMF-links. IEEE Photon. Technol. Lett. 24(1), 52–54 (2012)
8. Cinemre, I., Hacioglu, G.: A DCT/DST based fast OFDM method in IM/DD systems. IEEE Commun. Lett. 25(9), 3013–3016 (2021). https://doi.org/10.1109/lcomm.2021.3083672
9. Ouyang, X., et al.: Experimental demonstration of improved equalization algorithm for IM/DD fast OFDM. IEEE Photon. Technol. Lett. 27(16), 1780–1783 (2015). https://doi.org/10.1109/lpt.2015.2443076
10. Azim, A.W., et al.: Spectral and energy efficient fast-OFDM with index modulation for optical wireless systems. IEEE Commun. Lett. 24(8), 1771–1774 (2020). https://doi.org/10.1109/lcomm.2020.2989633
11. Hong, Y., et al.: SNR-Threshold based adaptive loading for PAM-fast-OFDM over optical wireless communications. In: 2018 Optical Fiber Communications Conference and Exposition (OFC), pp. 1–3 (2018)
12. Xu, T., Darwazeh, I.: Non-orthogonal narrowband internet of things: a design for saving bandwidth and doubling the number of connected devices. IEEE Internet Things J. 5(3), 2120–2129 (2018). https://doi.org/10.1109/jiot.2018.2825098
13. Nguyen, N.H., Berscheid, B., Nguyen, H.H.: Fast-OFDM with index modulation for NB-IoT. IEEE Commun. Lett. 23(7), 1157–1160 (2019). https://doi.org/10.1109/lcomm.2019.2917684
14. Liu, X., Darwazeh, I.: Quadrupling the data rate for narrowband internet of things without modulation upgrade. In: 2019 IEEE 89th Vehicular Technology Conference (VTC2019-Spring), pp. 1–5 (2019)
15. Anthony Haigh, P., Darwazeh, I.: Visible light communications: fast-orthogonal frequency division multiplexing in highly bandlimited conditions. In: 2017 IEEE/CIC International Conference on Communications in China (ICCC Workshops), pp. 1–8 (2017)
16. Salvestrini, J.P., et al.: Analysis and control of the DC drift in LiNbO3-Based mach–zehnder modulators. J. Lightwave Technol. 29(10), 1522–1534 (2011). https://doi.org/10.1109/jlt.2011.2136322
17. Yu, Y., et al.: Nonlinear equalizer based on absolute operation for IM/DD system using DML. IEEE Photon. Technol. Lett. 32(7), 426–429 (2020). https://doi.org/10.1109/lpt.2020.2978222
18. Jiang, T., Wu, Y.: An overview: peak-to-average power ratio reduction techniques for OFDM signals. IEEE Trans. Broadcast. 54(2), 257–268 (2008). https://doi.org/10.1109/tbc.2008.915770
19. Lee, T., Ochiai, H.: On limitation of clipping and filtering in IEEE 802.11g based wireless LAN system. In: WAMICON 2011 Conference Proceedings, pp. 1–5 (2011)
20. Qian, H., et al.: Adaptive postdistortion for nonlinear LEDs in visible light communications. IEEE Photon. J. 6(4), 1–8 (2014). https://doi.org/10.1109/jphot.2014.2331242
21. Mateo, C., et al.: Digital predistortion of a full-duplex Radio-over-Fiber mobile fronthaul link with feedback loop. In: 2017 13th International Wireless Communications and Mobile Computing Conference (IWCMC), pp. 1425–1430 (2017)
22. Vieira, L.C., Gomes, N.J.: Experimental demonstration of digital predistortion for orthogonal frequency-division multiplexing-radio over fibre links near laser resonance. IET Optoelectron. 9(6), 310–316 (2015). https://doi.org/10.1049/iet-opt.2014.0160
23. Ouyang, X., Zhao, J.: Single-tap equalization for fast OFDM signals under generic linear channels. IEEE Commun. Lett. 18(8), 1319–1322 (2014). https://doi.org/10.1109/lcomm.2014.2329486
24. Morgan, D.R., et al.: A generalized memory polynomial model for digital predistortion of RF power amplifiers. IEEE Trans. Signal Process. 54(10), 3852–3860 (2006). https://doi.org/10.1109/tsp.2006.879264
25. Ding, L., et al.: A robust digital baseband predistorter constructed using memory polynomials. IEEE Trans. Commun. 52(1), 159–165 (2004). https://doi.org/10.1109/tcomm.2003.822188
26. Vieira, L.C., et al.: Modeling and compensation of nonlinear distortion in direct-detection optical Fast-OFDM systems. In: 2022 13th International Symposium on Communication Systems, Networks and Digital Signal Processing (CSNDSP), pp. 168–173 (2022)
27. Chen, M., et al.: Experimental demonstration of real-time high-level QAM-encoded direct-detection optical OFDM systems. J. Lightwave Technol. 33(22), 4632–4639 (2015). https://doi.org/10.1109/jlt.2015.2458012
28. Gharaibeh, K.M.: Nonlinear Distortion in Wireless Systems: Modeling and Simulation with MATLAB. Wiley-IEEE Press (2012)
29. Vieira, L.C., et al.: Experimental demonstration of direct-detection optical fast-OFDM using memory polynomials. In: 2021 IEEE Latin-American Conference on Communications (LATINCOM), pp. 1–5 (2021)
30. Ghannouchi, F.M., Hammi, O., Helaoui, M.: Behavioral Modeling and Predistortion of Wideband Wireless Transmitters. John Wiley & Sons (2015)

How to cite this article: Vieira, L.C., et al.: Non-linear modelling and distortion compensation in optical Fast-orthogonal frequency division multiplexing systems. IET Optoelectron. 1–10 (2023). https://doi.org/10.1049/ote2.12097